Destruction of Biomass Tar Using a Gliding Arc Plasma Reformer

Young Nam Chun[#1], Seong Cheon Kim[#2], Kunio Yoshikawa[*3]

[1, 2#]BK21 Team for Hydrogen Production· Department of Environmental Engineering, Chosun University
#375, Seosuk-dong, dong-gu, Gwangju, 501-759, Rep. Korea.

[3*]Department of Environmental Science and Technology, Tokyo Institute of Technology
G5-8 4259 Nagatsuta, Midori-ku, Yokohama 226-8502, Japan

[1]ynchun@chosun.ac.kr, [2]chuneey@stmail.chosun.ac.kr, [3]yoshikawa.k.aa@m.titech.ac.jp

***Abstract*- The pyrolysis and gasification is energy conversion technology for biomass to produce synthetic gases for industrial use. The tar in the thermal decomposition gas from the pyrolysis or gasification process, however, damages synthetic gas facilities and causes operation trouble. A gliding arc plasma reformer for tar decomposition was developed to address the aforementioned problem. The performance in decomposition mechanism and characteristic was conducted for a pyrene as a surrogate of biomass tar. Parametric experiments were conducted for steam feed rate, input power, total gas amount, and input tar concentration. Through experimental results, decomposition efficiency, energy efficiency, reforming gas and carbon black concentration have been established. At optimal conditions, decomposition efficiency was 88.3%, while energy efficiency of 0.13 g/kWh was obtained. The higher heating value of the producer gas was 11,308 kJ/Nm^3 (excluding N_2) with carbon balance of 93.8%.**

Keywords*- *Gliding arc plasma; Tar; Pyrene; Decomposition efficiency; Pyrolysis; Biomass

I. INTRODUCTION

The technology converted into the energy from the waste resources, has been interested due to the depletion of the fossil energy and alternative energy development. Pyrolysis and gasification are widely acknowledged as promising conversion technology for the treatment of organic waste, sewage sludge in particular [1-4]. The producer gas generated in the pyrolysis and gasification of the biomass has tar like the pyrene which is the complicated hydrocarbon [3, 4]. As tar condenses at low temperature, it can cause clogging, pipeline corrosion, and aerosol formation during the post-production phase. Furthermore, if it enters the engine, it can block inlet channels, cooler, and filter element due to polymerization [5-7]. There have been a number of researches on tar removal using thermal cracking [8, 9], catalysis [6, 7, 10], etc. For thermal cracking, however, high reaction temperature of about 800^{o}C is needed that involves large energy consumption. Catalytic reactions have high affinity to sulfur, chlorine, and nitrogenous oxide that are major contaminants from biomass pyrolysis gasification. Also, tar can be deposited on the active area of the catalyst and badly compromise reaction efficiency that would require frequent regeneration of the active agent [11]. Compared to pyrolysis and catalysis, plasma discharge shows higher removal efficiency due to radical formation. To make plasma technology practically feasible, however, the problems of short lifetime and power consumption should be solved.

In this study, gliding arc plasma has been selected for removing tar formed in pyrolysis gasification of biomass. The 3-phase AC gliding arc plasma applied to the tar removal technology is easy to control reaction and low cost of power supply. In addition, it has the high energy efficiency and the decomposition efficiency. Therefore, an application is effective at a tar removal technology as a new method.

Thus, pyrene was selected for simulations for determining corresponding removal characteristics. To evaluate energy efficiency of the gliding arc plasma process and pyrene decomposition efficiency, parametric experiments have been carried out for steam feed, input power, total gas amount, and input tar concentration.

II. EXPERIMENTAL EQUIPMENT AND METHOD

A. Experimental Equipment and Configuration

Fig. 1 shows the experimental equipment for tar removal. The equipment consists of the gliding arc plasma reformer, steam feeding line, tar feeding line, power supply equipment, measuring & analysis line and control &monitoring system.

3 blade electrodes (2 mm width, 95 mm length, 2 mm thick) are installed in 120° from the center off gliding arc plasma reactor. The distance between the electrodes is 3 mm. Ceramic (Al_2O_3, wt 96%) is used to fix reactor insulator and electrode. In addition, the diameter of the gas nozzle is 1.5 mm. The outer shell of the plasma reactor was quartz pipe (55 mm diameter, 200 mm length) that serves as an insulator and enables to check the interior at a time.

Steam feeding line consisted of steam generator and water pump (Model STEPDOS03, KNF, Switzerland.) distilled water is filled into the water tank, and supplied to the steam generator using a water pump, which controlled the flow for steam amount.

Tar feeding line consisted of 2 MFCs (Model F201AC-FAC-22-V, BRONKHOST, Netherlands, Model M3030V, LINETECH, Korea) for providing specific amount of nitrogen and tar generator. Tar generator used mantle heater to heat the glass container with solid pyrene. By controlling

the flow rate of the nitrogen, the amount of tar can be adjusted.

The power supply equipment consisted of power supply (Model UAP-15K1A, Unicon tech., Korea), high voltage probe (Model P6015, Tektronix, USA), low current probe (Model A6303, Tektronix, USA), and oscilloscope (Model TDS-3052, Tektronix, USA). The power supply unit can provide 15 kW 3-phase AC power (voltage: 15 kV, AC: 1A) to the gliding arc plasma reformer, voltage and current probes are used to measure the power.

Measuring & Analysis line consisted of the sampling unit and analysis equipments. Sampling unit was made of soot filter (Model LS-25, Advantec, Japan), impingers, isothermal bath, and chiller (Model ECS-30SS, Eyela Co., Japan). Analysis equipments included GC-FID (Model GC-14B, SHIMADZU, Japan) for tar analysis and GC-TCD (Model CP-4900, Varian, Netherland) for gas analysis.

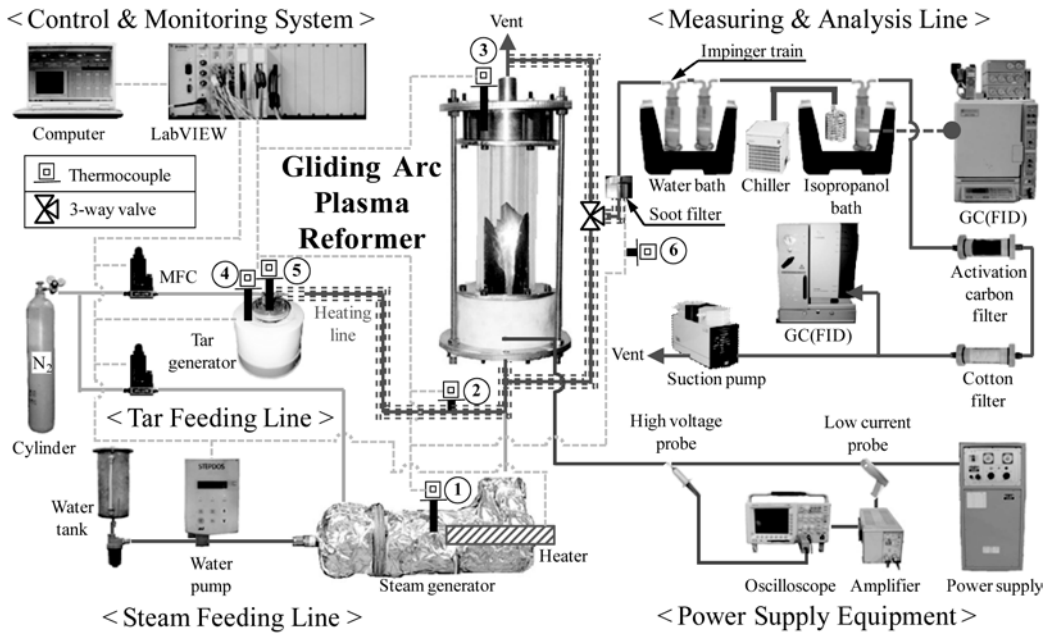

Fig. 1 Experimental facility

Control & Monitering system was made of LabVIEW (Model LabVIEW 8.6, National Instrument, USA) for MFC, water pump, and heater controller. Changes in temperature, steam feed, and nitrogen flow rate are continuously monitored.

B. Experimental Method

Fig. 2 shows initial and stabilization temperature in gliding arc plasma. Experiment is carried out at 500°C at steam generator. For pyrene, the melting point is about 148°C and the boiling point is 404°C. Therefore, temperature of the mantle is maintained in-between at 260°C. The heating line up to the plasma reactor is heated up to 400°C using tape heater. The sampling line and soot filter are kept at 150°C and 120°C, respectively. Nitrogen is supplied into the tar generator and steam generator, and it was introduced to plasma reformer by mixing nitrogen and steam at steam generator. The temperature at the tar generator is kept for 2 hours for stabilization to take place, and tar input concentration is analyzed at the inlet of the gliding arc plasma reactor. After plasma reaction, tar, carbon black, and reforming gases were analyzed at the gliding arc plasma reformer outlet.

Table 1 shows parametric test conditions, range, and reference conditions.

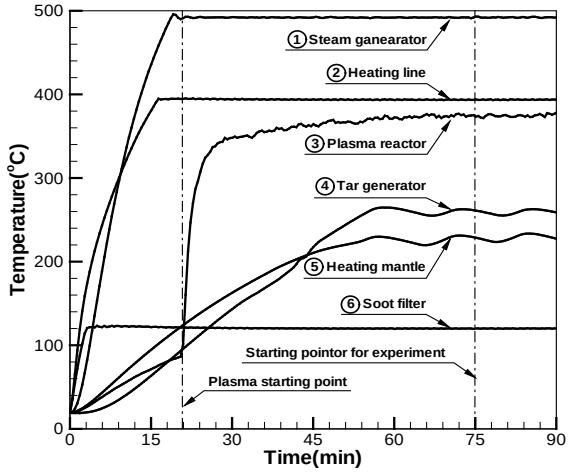

Fig. 2 Initial operating conditions in the gliding arc plasma reformer

C. Sample Analysis and Method of Tar, and Carbon Black

Tar sampling is made using wet sampling measurement. Wet sampling is connected to the inlet and the outlet of the gliding arc plasma reformer and consists of 3 impingers, 2 isothermal baths, and filter. At the first isothermal bath maintained below 20°C and 50 mL of isopropyl alcohol is filled in 2 impingers. In the second isothermal bath maintained below -20°C using a chiller and one empty impinger is installed. For the installed impingers, tar and

moisture from gliding arc plasma reformer are absorbed and condensed. Samples are collected for 20 minutes in 3 L/min of rate using the metering pump (Model N-820.3FT 18, KNF, Switzerland). The collected solution is analyzed using GC-FID, and column for tar analysis was RTX-5 (RESTEK, USA; 30 m - 0.53 mm id, 0.5 μm film thickness). Analysis condition was set to be 320°C for 2 minutes after maintaining 45°C for 2 minutes and heating with 7°C/min. The temperatures of detector and injector were 340°C and 250°C, respectively.

TABLE I EXPERIMENTAL CONDITIONS FOR PARAMETRIC RANGE AND REFERENCE CONDITIONS

Experimen-tal conditions	Steam flow rate (L/min)	Specific energy input (kWh/m^3)	Total gas flow rate (L/min)	Input tar Concentra-tion (g/Nm^3)
Range	0~1.57	0.91~1.21	7.2~24.1	0.1~0.61
Reference value	0.37	0.91	12.05	0.13

Gas sampling is conducted at the same time as tar is sampled. The gas going through the impinger is analyzed with GC-TCD after passing the cotton filter and the activated carbon filter. Cotton filter and activated carbon filter are installed to prevent the inflow of residual tar component to GC. For gas analysis MolSieve 5A PLOT column is used, which can analyze H_2, CO, CH_4, O_2, and N_2 and PoraPLOT Q for CO_2, C_2H_4, and C_2H_6.

Carbon black sampling is made along with tar sampling. Glass filter (Model GA-100, Advantec, Japan) is installed at inside the filter and weight difference before and after sampling is measured.

D. Data Analysis

Tar decomposition efficiency, energy efficiency, specific energy input, and carbon balance in gliding arc plasma reformer can be calculated according to Eqs. (1) ~ (4).

Tar decomposition efficiency can be expressed as Eq. (1).

$$\eta_t\,(\%) = \frac{[TC]_{inlet} - [TC]_{outlet}}{[TC]_{inlet}} \times 100 \quad (1)$$

Where, $[TC]_{inlet}$ is input tar concentration (g/Nm^3), and $[TC]_{outlet}$ is effluent concentration for tar (g/Nm^3).

Energy efficiency can be expressed as Eq. (2).

$$\eta_e(gkW^{-1}h^{-1}) = \frac{[TC]_{removal} \times Q}{IP} \quad (2)$$

Where, $[Tar]_{removal}$ is the concentration of the removed tar (g/Nm^3), and Q is the amount of the input gas entering reactor. IP is plasma input power (kW).

Specific energy input (SEI) is expressed as Eq. (3).

$$SEI(kWhm^{-3}) = \frac{IP}{Q} \quad (3)$$

Carbon balance equation can be expressed as Eq. (4).

$$Carbon\ balance\,(\%) = \frac{[CO] + [CO_2] + [CH_4] + 2[C_2H_4] + 2[C_2H_6] + CB}{A([TC]_{inlet} - [TC]_{outlet})} \times 100 \quad (4)$$

Where, [CO], $[CO_2]$, $[CH_4]$, $[C_2H_4]$ and $[C_2H_6]$ are concentrations of each component (g/Nm^3), and CB is the concentration of carbon black (g/Nm^3). A is carbon constant. (16 for pyrene)

E. Data Analysis

Pyrene removal mechanism in the gliding arc plasma reformer can be described as follows. In the gliding arc plasma reformer cracking (5) and carbon black formation reactions (6) dominate [12].

- Cracking reaction

$$pCnHx \rightarrow qCmHy + rH_2 \quad (5)$$

- Formation reaction of carbon black

$$CnHx \rightarrow nC + (x/2)H_2 \quad (6)$$

With steam introduced into the gliding arc plasma reformer, radical formation/conversion/ depletion and reaction mechanism for carbon black can be expressed as Eqs. (7) ~ (11) [11, 13].

- Radical formation reaction

$$e + H_2O \rightarrow e + H + OH \quad (7)$$

- Radical conversion reaction

$$OH + tar \rightarrow Products \quad (8)$$

- Radical depletion reaction

$$OH + CO \rightarrow CO_2 + H \quad (9)$$

- Carbon black conversion reaction

$$C_x + OH \rightarrow C_{x-1} + CO + 1/2H_2 \quad (10)$$

$$C_x + 2OH \rightarrow C_{x-1} + CO_2 + H_2 \quad (11)$$

Gas reaction after tar reaction due to plasma and OH radical can be divided into steam conversion (12) and steam reforming reaction (13) [14].

- Steam conversion reaction

$$CO + H_2O \rightarrow CO_2 + H_2$$

TABLE II OPTIMUM CONDITIONS AND EXPERIMENTAL RESULTS

Optimum case						
Conditions	Steam flow rate (L/min)	Specific energy input (kWh/m^3)	Total gas flow rate (L/min)	Input tar concentration (g/Nm^3)		
Value	0.5	0.91	12.05	0.13		
Experiment results						
Result	Gas composition after the reformer (%, N_2 excluded)	Carbon black	Carbon balance	Higher heating value	Decomposition efficiency	Energy Efficiency

	H_2	CO	CO_2	CH_4	C_2H_4	C_2H_6	(g/Nm^3)	(%)	(kJ/Nm^3)	(%)	(g/kWh)
	81.0	5.2	13.0	0.8	0	0	0.007	93.8	11,308	88.3	0.13

$$\Delta H = 131.3 \text{ kJ/mol} \quad (12)$$

- Hydrocarbon steam reforming reaction

$$CnHm + nH_2O = nCO + (n + m/2)\, H_2 \quad (13)$$

III. RESULTS AND DISCUSSION

Optimal condition and the experimental results are shown in Table II. Under optimal conditions the decomposition efficiency for pyrene was 88.3%, and the energy efficiency was 0.13 g/kWh. Table shows gas concentration after pyrene decomposition. Higher heating value was found to be 11,308 kJ/Nm^3 with carbon balance of 93.8%. The reason why carbon balance is below 100% is that carbon black is deposited inside the reactor and there is no consideration on the formed elements due to HCN and CN from nitrogen gas in plasma discharge [15].

A. Results of Parametric Experiments

1) Input Steam Flow Rate:

Fig. 3 shows the change in steam flow rate. When total gas amount is maintained as 12.05 L/min along with 0.91 kWh/m^3 of SEI, experiment was conducted to evaluate the impact of change in steam flow rate. In case that there is no steam feed, decomposition efficiency was 76.4%. Therefore, decomposition efficiency was higher due to cracking reaction of pyrene and formed electrode/active chemical species during plasma discharge. Pyrene was converted to hydrogen, carbon black, and hydrocarbons according to Eqs.

(5) and (6), plasma cracking reaction and carbon black formation reaction. If steam flow rate was increased, decomposition efficiency at 0.5 L/min displayed the maximum of 88.3%. Once steam flow rate was excessively introduced at higher than 0.5 L/min, decomposition efficiency was decreased. At 1.57 L/min of steam flow rate, decomposition efficiency was 66.5%. When steam is introduced to plasma reformer, H/OH radical is formed according to Eq. (7). If steam amount to reformer is increased up to 0.5 L/min, formed OH radical will react with pyrene for decomposition. However, higher than 0.5 L/min of steam flow rate limited the electron density of plasma discharge, and steam cooled activated chemical species down. These were decreased decomposition efficiency of pyrene [16].

For energy efficiency, steam flow rate between 0 L/min and 0.062 L/min shows the increased amount of removed pyrene due to OH radical, and the maximum value of 0.145 g/kWh was found at 0.062 L/min. Steam flow rate between 0.062 L/min and 0.5 L/min exhibited the slight decrease in energy efficiency due to the decreased removal amount.

For more than 0.5 L/min of steam flow rate, further drop in decomposition efficiency for pyrene was displayed due to restricted electron density in plasma and cooling of activated chemical species. In addition, dilution by input steam decreased the input concentration of pyrene, and significant reduction of energy efficiency was found. For carbon black, cracking reaction of pyrene under plasma discharge showed 0.025 g/Nm^3 for without steam. For more than 0.37 L/min of steam flow rate, carbon black was reduced to 0 g/Nm^3. According to Eqs. (10) and (11), formed OH radical converted carbon black into carbon monoxide and carbon dioxide.

In formed gases, hydrogen, carbon monoxide, carbon dioxide, methane, ethane, and ethylene were found. Without steam, 0.079% of hydrogen, 0.19% of methane, 0.003% of ethane, and 0.001% of ethylene was formed, respectively. Hydrogen concentration was increased from 0.079% to 1.06% along with increase in steam flow rate due to cracking reaction of pyrene and carbon black conversion for OH radical. Carbon monoxide also showed the increase to 0.029% for 0.37 L/min of steam flow rate. For 1.56 L/min of steam flow rate, Carbon monoxide was significantly reduced to 0.007%. Reaction of carbon black due to the initial OH radical and steam reforming reaction for hydrocarbon formed carbon monoxide. However, increased amount of steam converted carbon monoxide to carbon dioxide due to steam conversion reaction. Carbon dioxide showed the increase up to 0.147% along with increase in steam flow rate. Therefore, the OH radical reacted with the carbon black and was converted to the carbon monoxide.

And the steam conversion reaction increased the concentration of carbon dioxide. Methane, ethane, and ethylene, displayed the reduction in concentration along with increase in steam flow rate. Hydrocarbon was formed from initial cracking

reaction, and it was converted into hydrogen and carbon monoxide according to Eq. (12).

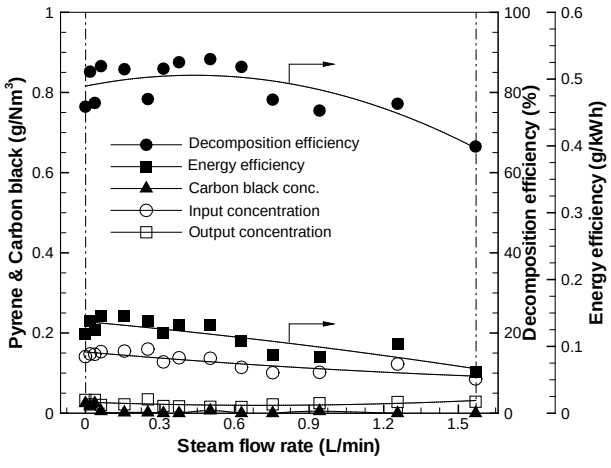

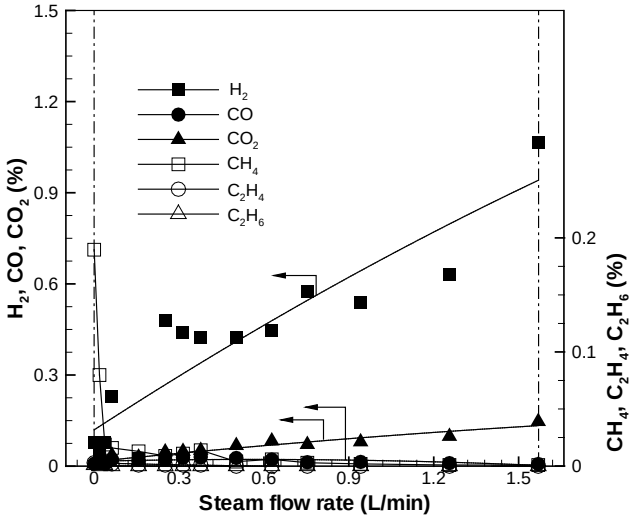

Fig. 3 The effect of the various steam flow rate

2) Input Power:

Fig. 4 shows experimental results according to input power. The test is conducted when the total gas amount is fixed at 12.05 L/min, and steam flow rate is 0.37 L/min. When specific energy input (SEI) increases from 0.91 to 1.21kWh/m^3, tar decomposition efficiency increases from 87.5% to 94.1%. Along with increase in SEI, the amount of electron transfers between the electrodes seems to be enhanced to facilitate tar cracking reaction and OH radical formation [17]. Even with increase in SEI, however, average energy efficiency is 0.13 g/kWh. This can be explained by the fact that energy efficiency goes down with increased efficiency of tar removal. Carbon black via formation of OH radical due to steam feed was not collected less than 1.14 kWh/m^3, of SEI. Above 1.14 kWh/m^3 a small amount of carbon black (0.0016 g/m^3) was collected. The formation of carbon black is improved with higher tar decomposition efficiency via cracking reaction.

When SEI further increases to 1.21 kWh/m^3, the amount of produced hydrogen, carbon monoxide,

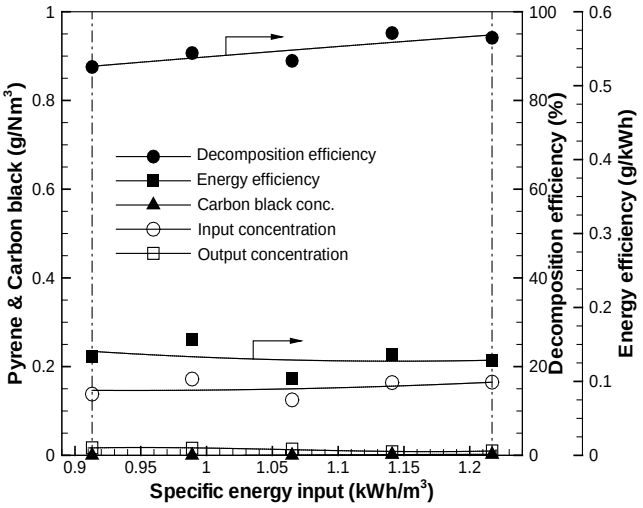

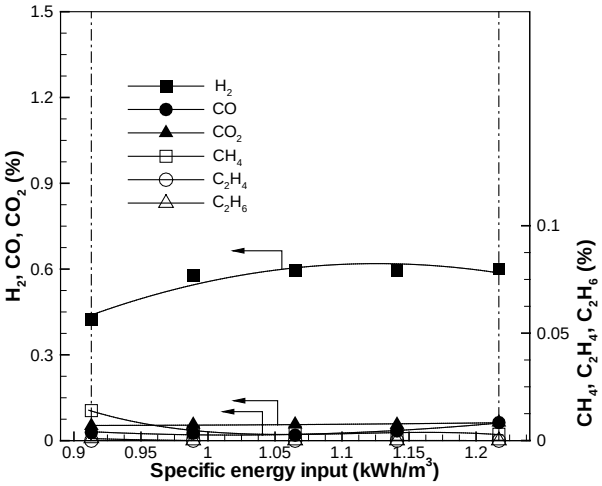

Fig. 4 The effect of specific energy input

and carbon dioxide increased to 0.599%, 0.062%, and 0.064%, respectively, according to Eqs. (5), (10), (11), (12), and (13). Methane, however, showed the opposite trend of decreasing from 0.014% to 0.0003%.

3) Total Gas Amount:

Fig. 5 shows the effect of total gas amount. The test is conducted at the following fixed conditions: steam feed 0.37 L/min, SEI 0.91 kWh/m^3, input tar concentration 0.13 g/Nm^3. Less than 7 L/min of total gas amount, instable discharge was developed, and plasma formation cycle would be slow due to low velocity of gas rate from nozzle. Moreover, at the Total gas flow rate above 25 L/min nonhomogeneous mix of nitrogen and pyrene was established at the inlet of the nozzle along with increased pressure. Therefore, test range of total gas flow rate was set to 7.2 ~ 24.1 L/min.

The total gas flow rate showed the maximum decomposition efficiency of 87.5% in 12.05 L/min, and then the decomposition efficiency decreased. When total gas flow rate increases to 12.05 L/min, plasma discharge is stabilized, and its formation cycle becomes faster to induce higher decomposition efficiency. At the 12.05 L/min or above, the reaction time between pyrene and the plasma discharge area and contact area are decreased by the increase of the flow velocity. Therefore, the decomposition efficiency of a pyrene reduced. Therefore, reactions of activated electron in plasma discharge and pyrene decomposition by OH radical and activated chemical species were decreased [18, 19]. Regarding to energy efficiency, the maximum value of 0.18 g/kWh was obtained when total gas flow rate increased to 19.4 L/min. Further increase in total gas amount to 24.1 L/min resulted in reduced energy efficiency. Because the energy efficiency was the proportional relation with total gas flow rate by the Eq. (2), although the removal efficiency reduced by the increasing of total gas flow rate, the energy efficiency showed the result of increasing. For carbon black, due to the formation of consistent formation of OH radical, it was not collected in test range according to Eqs. (10) and (11). Hydrogen is formed not only by pyrene cracking, but also reaction termination of radical according to Eq. (9).

Although the decomposition reaction of the tar reduced in the Eq. (12), the tendency that the concentration of the hydrogen was on the increase, was shown. Carbon monoxide concentration decreases from 0.05% to 0.02% when total gas flow rate increases. Carbon dioxide showed, however, the opposite trend of increasing from 0.036% to 0.055%. This can be explained by the fact that the carbon formed in initial cracking reaction is converted to carbon monoxide according to Eq. (10), and the corresponding carbon monoxide is oxidized to carbon dioxide via Eqs. (9) and (12). Ethylene and ethane are not formed while the average concentration of methane is 0.005%.

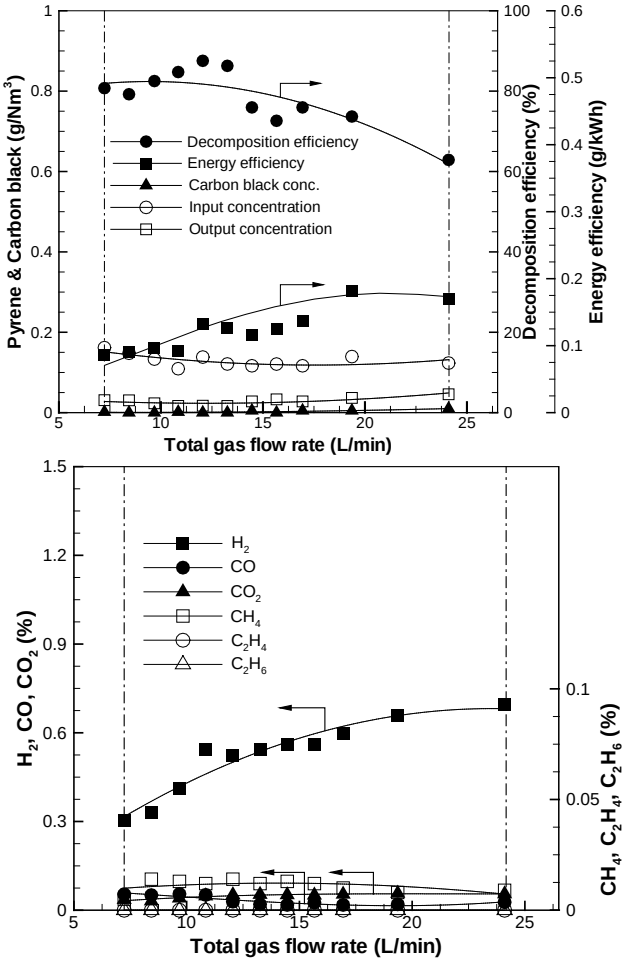

Fig. 5 The effect of total gas flow rate

4) Input Tar Concentration:

Fig. 6 shows the effect of input pyrene concentration. Other test variables value follows: steam feed 0.37 L/min, SEI 0.91 kWh/m^3, and total gas amount 12.05 L/min. At that, input pyrene concentration changes from 0.12 to 0.61 g/Nm^3.

The highest decomposition efficiency of pyrene of 89.1% was obtained at 0.21 g/Nm^3 of input pyrene concentration. The decomposition efficiency showed a maximum 89.1% when the

input concentration of a pyrene was 0.21g / Nm^3. Because of fixed SEI and steam feed, the amount of electron and active chemical species in plasma is limited, and decomposition efficiency decreases with the increase of pyrene input concentration. The change of the input concentration indicates the important influence in the energy efficiency of the plasma. Energy efficiency linearly depends on input concentration. The maximum energy efficiency of 0.45 g/kWh is obtained at input concentration of 0.49 g/Nm^3. This is related to increase in pyrene removal even though of reduced decomposition efficiency. For carbon black, fixed amount of OH radical and activated chemical species induces unreacted carbon black for 0.21 g/Nm^3 above of input concentration. It was resulted as collected carbon black. When input concentration increases to 0.49 g/Nm^3, the amount of carbon black increased to 0.217 g/Nm^3. For gas species, the concentration of hydrogen, carbon monoxide, carbon dioxide, methane, ethylene, and ethane increased with pyrene input concentration. At input concentration of 0.61 g/Nm^3, the corresponding concentration of gas species was 1.31%, 0.14%, 0.057%, 0.011%, 0.006%, and 0.009%, respectively. The input concentration of pyrene was on the increase and the decomposition efficiency was reduced. However, the removal amount of a pyrene increased continuously. Therefore, the concentration of the corresponding gas is considered to be increased according to Eqs. (5), (6), (10), and (11).

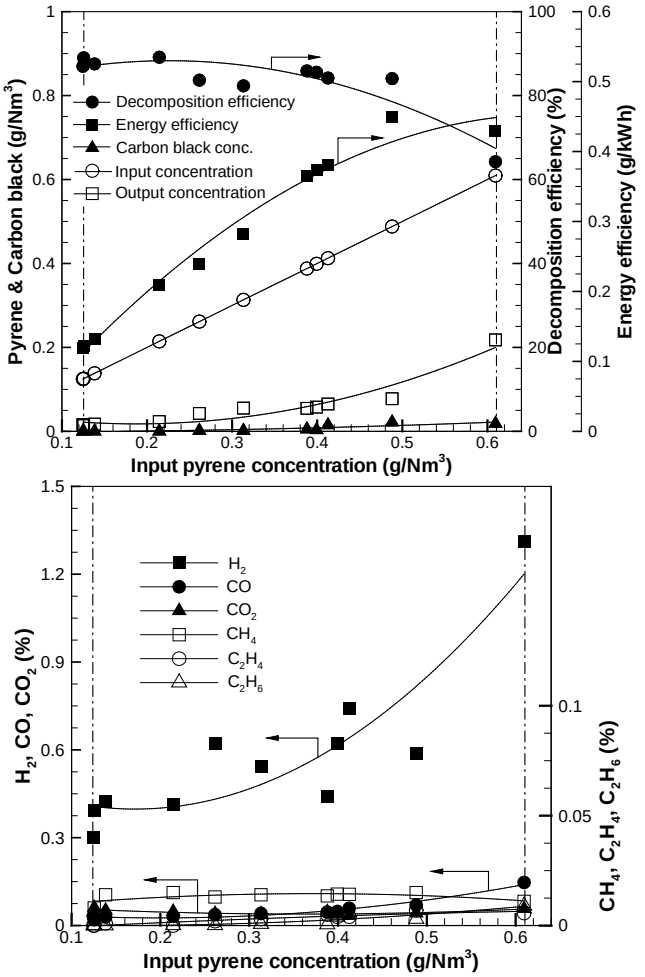

Fig. 6 The effect of the input pyrene concentration

IV. CONCLUSIONS

In this study, gliding arc plasma reformer was designed to remove tar from biomass pyrolysis. As a representative tar, a pyrene was selected. At the optimal conditions, decomposition efficiency of pyrene was 88.3% at 0.13 g/kWh of energy efficiency. Higher heating value for formed gas from pyrene decomposition was 11,308 kJ/Nm^3 (excluding N_2), and carbon balance was 93.8%.

Among reference conditions, 0 L/min of steam supply showed 76.4% of tar removal efficiency due to cracking reaction in gliding arc plasma reforming. In addition, carbon black was formed. Below of 0.5 L/min of steam flow rate, formation of OH radical from steam displayed 88.3% of tar removal efficiency. Increase in steam flow rate causes reduction of electron density by plasma, and decreases the amount of activated chemical species, such as OH radical. This eventually reduces the decomposition efficiency of pyrene.

In reference conditions, 1.21 kWh/m^3 of SEI showed 94.1% of pyrene decomposition efficiency. Increment in SEI facilitates electron transfer between electrodes and the reaction between OH radical and tar for higher removal efficiency. However, energy efficiency was averaged to be 0.13 kWh/m^3 due to increased plasma supply power.

10.05 L/min of total gas amount displayed the maximum decomposition efficiency at 87.5%. However, decomposition efficiency was decreased due to less reaction between pyrene and activated chemical species, OH radical, in plasma discharged area along with the increment of total gas amount. The maximum energy efficiency, 0.18 g/kWh, was achieved at 24 L/min of total gas amount.

Regarding to input pyrene concentration, 0.12 g/Nm^3 showed 87.5% of decomposition efficiency. Due to limitation on the amount of formed electron and activated chemical species in plasma, increase in input pyrene concentration induced decrease in decomposition efficiency. For 0.61 g/Nm^3 of input pyrene concentration, energy efficiency was increased up to 0.43 g/kWh because of increased amount of pyrene removal.

Therefore, tar from pyrolysis and gasification of biomass via gliding arc plasma reformer can be effectively removed, and it is converted to syngas with hydrogen concentration due to additional reaction with steam.

ACKNOWLEDGEMENT

This research was supported by Basic Science Research Program through the National Research Foundation of Korea (NRF) funded by the Ministry of Education, Science and Technology (2010-0004156).

REFERENCES

[1] L. Shen and D. K. Zhang, "Low-temperature pyrolysis of sewage sludge and putrescible garbage for fuel oil production," *Fuel*, vol. 84, pp. 809-815, 2005.

[2] I. Fonts, E. Kuoppala, and A. Oasmaa, "Physicochemical Properties of Product Liquid from Pyrolysis of Sewage Sludge," *Energy&Fuels*, vol. 23, pp. 4121-4128, 2009.

[3] M. Aznar, S. M. Anselmo, J. J. Manya, and M. B. Murillo, "Experimental Study Examining the Evolution of Nitrogen Compounds during the Gasification of Dried Sewage Sludge," *Energy&Fuels*, vol. 23, pp. 3236-3245, 2009.

[4] T. Phuphuakrat, N. Nipattummakul, T. Namioka, and S. Kerdsuwan, "Characterization of tar content in the syngas produced in a downdraft type fixed bed gasification system from dried sewage sludge," *Fuel*, vol. 89, pp. 2278-2284, 2010.

[5] L. Devi, K. J. Ptasinski, and F. J. J. G. Janssen, "A review of the primary measures for tar elimination in biomass gasification processes," *Biomass and Bioenergy*, vol. 24, pp. 125-140, 2003.

[6] L. Devi, K. J. Ptasinski, and F. J. J. G. Janssen, "Pretreated olivine as tar removal catalyst for biomass gasifiers: investigation using naphthalene as model biomass tar," *Fuel Processing Technology*, vol. 86, pp. 707-730, 2005.

[7] C. Li, D. Hirabayashi, and K. Suzuki, "Development of new nickel based catalyst for biomass tar steam reforming producing H_2-rich syngas," *Fuel Processing Technology*, vol. 90, pp. 790-796, 2009.

[8] K. Zhang, H. T. Li, Z. S. Wu, and T. Mi, "The Thermal Cracking Experiment Research of Tar Model Compound," *In: 2009 International Conference on Energy and Environment Technology*, 2009, p. 655-659.

[9] L. Fagbemi, L. Khezami, and R. Capart, "Pyrolysis products from different biomasses: application to the thermal cracking of tar," *Applied Energy*, vol. 69, pp. 293-306, 2004.

[10] H. Noichi, A. Uddin, and E. Sasaoka, "Steam reforming of naphthalene as model biomass tar over iron-aluminum and iron-zirconium oxide catalyst catalysts," *Fuel Processing Technology*, vol. 91, pp. 1609-1616, 2010.

[11] A. J. M. Pemen, S. A. Nair, K. Yan, E. J. M. Van Heesch, K. J. Ptasinski, and A. A. H. Drinkenburg, "Pulsed Corona Discharges for Tar Removal from Biomass Derived Fuel Gas," *Plasmas and Polymers*, vol. 8, pp. 209-224, 2003.

[12] N. Tippayawong and P. Inthasan, "Investigation of Light Tar Cracking in a Gliding Arc Plasma System," *International Journal of Chemical Reactor Engineering*, vol. 8, pp. 1-16, 2010.

[13] C. M. Du, J. H. Yan, X. D. Li, B. G. Cheron, X. F. You, Y. Chi, M. J. Ni, and K. F. Cen, "Simultaneous Removal of Polycyclic Aromatic Hydrocarbons and Soot Particles from flue Gas by Gliding arc Discharge," *Treatment. Plasma Chemistry and Plasma Processing*, vol 26, pp. 517-525, 2006.

[14] M. A. Rakib, J. R. Grace, S. S. E. H. Elnashaie, C. J. Lim, and Y. G. Bolkan, "Kinetic simulation of a compact reactor system for hydrogen production by steam reforming of higher hydrocarbons," *The Canadian Journal of Chemical Engineering*, vol. 86, pp. 403-412, 2008.

[15] L. Yu, X. Li, X. Tu, Y. Wang, S. Lu, and J. Yan, "Decomposition of Naphthalene by dc Gliding Arc Gas Discharge," *The Journal of Physical Chemistry A*, vol. 114, pp. 360-368, 2009.

[16] C. M. Du, J. H. Yan, and B. Cheron. "Decomposition of toluene in a gliding arc discharge plasma reactor," *Plasma Sources Science and Technology*, vol. 16, pp. 791-797, 2007.

[17] T. Sreethawong, P. Thakonpatthanakun, and S. Chavadej, "Partial oxidation of methane with air for synthesis gas production in a multistage gliding arc discharge system," *International Journal of Hydrogen*, vol. 32, pp. 1067-1079, 2007.

[18] W. Mista and R. Kacprzyk, "Decomposition of toluene using non-thermal plasma reactor at room temperature," *Catalysis Today*, vol. 137, pp. 345-349, 2008.

[19] Z. Bo, J. Yan, X. Li, Y. Chi, and K. Cen, "Scale-up analysis and development of gliding arc discharge facility for volatile organic compounds decomposition," *Journal of Hazardous*, vol. 155. pp. 494-501, 2008.